www.sphinxsai.com

ChemTech

International Journal of ChemTech Research
CODEN(USA): IJCRGG ISSN : 0974-4290
Vol.1, No.4, pp 1109-1124, Oct-Dec 2009

Computation and interpretation of vibrational spectra on the structure of Nitrazepam using semi-empirical and density functional methods

S.Gunasekaran[1], R.ArunBalaji[2*], S.Kumaresan[3] , G. Anand[3], & M.VivekAnand[2]
[1]Registrar, Periyar University, Salem, India.
[2]Department of Physics, Rajiv Gandhi College of Engineering, Sriperumbudur 602 105. , India.
[3]Department of Physics, Arulmigu Meenakshi Amman College of Engineering, Vadamavandal , India.

Corres.author: aaraay@gmail.com

Abstract: Nitrazepam is chemically known as 9-Nitro-6-phenyl-2, 5-diazabicycio (5, 4, 0) undeca-5, 8, 10, 12-tetraen-3-one. The vibrational (IR) spectrum of Nitrazepam were investigated by the density functional BLYP/6-31G(d)//B3LYP/6-31G(d) and semi empirical AM1, PM3 methods in this work. The FTIR and FTRaman spectra of Nitrazepam were recorded in the region 4000 – 500 cm^{-1} and 4000 – 100 cm^{-1}. With the help of the specific scaling procedure, the observed vibrational wavenumbers in FTIR and FTRaman spectra were analyzed and assigned to different normal modes of the molecule. Most of the modes have wave numbers in the expected range and are also in good agreement with computed scaled values. The observed IR and Raman spectra agree well with the theoretically predicted spectra. The experimental geometry and wave numbers are compared with the results of our theoretical calculations. The theoretical spectrograms for the IR spectrum were also constructed in BLYP and B3LYP levels.

Keywords. FTIR; FT-Raman; semiempirical, density functional theory; Nitrazepam.

1. Introduction

Recently, the clinical use of 1, 4-benzodiazepines (BDZ) as anxiolytic, anticonvulsant, sedative-hypnotic and muscle relaxant agents has increased enormously (1-6). After the first synthesis of the prototypical agents chlorodiazepoxide and diazepam, thousands of benzodiazepine congeners have been synthesized and studied at enormous laboratories (7-9). However, the molecular mechanism of their activity remains to be clarified. The discovery of stereospecific, high affinity BDZ binding sites in mammal brains that are capable of being saturated, has rekindled new interest in this field. Nitrazepam is a derivative of benzodiazepine had more prominent anticonvulsant activity than other benzodiazepines. Nitrazepam has been shown to actually increase Rapid-eye movement (REM) sleep. It induces bedtime sleep in 20-30mins with duration of up to 8hrs (10, 11). Nitrazepam is chemically known as 9-Nitro-6-phenyl-2, 5-diazabicycio (5, 4, 0) undeca-5, 8, 10, 12-tetraen-3-one. A quantitative structure-activity relationship (QSAR) study was carried out on over 50 BZD with a variety of substituents. Using CNDO/2 methodology and calculated values for dipole moment and net charge on the carbonyl oxygen, the data of several different in vivo tests has been analyzed (12-15). Conformational and electronic properties of 21 benzodiazepines were calculated by using empirical energy and semiempirical molecular orbital methods (16-18). Neville et al., (19) studied infrared and Raman spectra of delorazepam, fludiazepam flurazepam and tetrazepam and also reported the band assignments. Gunasekaran et al (20) reported the normal co-ordinate analysis of Nitrazepam using Wilson's F-G matrix. They have also attempted band assignments.

Literature survey reveals that to the best of our knowledge, no Density functional theory/Semiempirical frequency calculations for Nitrazepam have been reported so far the frequency assignments. Therefore, the present investigation was undertaken to study the vibrational spectra of this molecule completely and to identify the various normal modes with greater wave number accuracy. Density functional theory (DFT) and semiempirical (AM1, PM3)

calculations have been performed to support our wave number assignments.

The main aim of the present work is to find effective theoretical methods that would offer a higher certainty of finding molecular parameters and vibrational wave numbers. The calculated harmonic frequencies are usually higher than the corresponding experimental quantities, due to a combination of electron correlation effects and basis set deficiencies. In density functional theory (DFT) some correlation effects are taken into account through the effective exchange-correlation potential. Becke's three parameter exchange functional (B3-LYP) and Becke's exchange functional in combination with the Lee, Yang and Parr (LYP) correlation functional (BLYP) were the most widely used for molecular calculations by a fairly large margin (21, 22).

2. Experimental

The compound dacarbazine was purchased from Messrs Sigma–Aldrich Chemical Company, USA with more than 98% purity and was used as such without further purification to record FTIR and FTRaman spectra. The FTIR spectrum of the compound was recorded in the region 4000–400 cm^{-1} in evacuation mode on Bruker IFS 66V spectrophotometer using KBr pellet technique (solid phase) with 4□0 cm^{-1} resolution. The FT Raman spectrum was recorded using 1064 nm line of Nd : YAG laser as excitation wavelength in the region 3500–100 cm^{-1} on Bruker IFS 66V spectrometer equipped with FRA 106 FT Raman module accessory. FTIR and FTRaman spectra of Nitrazepam are presented in the figs 1 and 2 respectively.

3. Computational details

The entire calculations were performed at BLYP and B3LYP levels on a Pentium IV/11.6 GHz personal computer using Gaussian 03w (24) program package, invoking gradient geometry optimization. Initial geometry (23) generated from standard geometrical parameters was minimized without any constraint in the potential energy surface at BLYP and B3LYP levels, adapting the standard 6-31G(d) basis set. The optimized structural parameters were used in the vibrational frequency calculations at the BLYP and B3LYP levels to characterize all stationary points as minima. Then vibrationally averaged nuclear positions of Nitrazepam were used for harmonic vibrational frequency calculations together with intensities and force constants. Semiempirical Austin Model 1 (AM1) (25) and Parametric Method (PM3) (26) were also used for comparison. By combining the results of the Chemcraft program (30) with symmetry coordinates, vibrational frequency assignments were made with a high degree of accuracy. However, the defined coordinate form complete set and matches quite well with the motions observed using Chemcraft program.

4. Results and discussion

4.1 Geometric parameters

In the structure of Nitrazepam, seven membered heterocycle which is having two nitrogen and three double bonds named diazepine fused with benzene ring having a nitro group at the fifth position of the ring and a phenyl ring which lies approximately perpendicular to each other. Fig. 3 presents the geometry of the molecule optimized using DFT method at the B3LYP/6-31G(d) level. The optimized geometrical parameters determined using density functional and semi empirical AM1, PM3 methods are collected in Table 1. In the last column of Table 1, the experimental data of the molecule is also included. As discussed by Johnson et al (27) the BLYP functional leads to bond lengths which are systematically too long. The B3LYP method leads to geometry parameters which are much closer to experimental data (28, 29). A statistical treatment of these data (see at the bottom of Table 8.1) shows that for the bond lengths B3LYP/6-31G(d) is slightly better than the BLYP/6-31G(d) geometry. The correlation coefficient for DFT methods were bigger than 0.9944, whereas for semi empirical methods it were lowest than 0.971. Electron correlation is important for on the overall geometry of the complete molecular model geometrical parameters. The agreement between the calculated and the experimental bond angles is not as good as that of the bond lengths. The largest change between calculated and experimental bond angles are found in the N_{20}-C_{21}-H_{31} angle which varying from 111° (optimized) to 101° (in experimental).

4.2 Infrared spectra

With this assumed structural model, the molecule belongs to C_1 point group and has 90 normal modes of fundamental vibrations. To our best knowledge, no complete vibrational analyses have been reported for Nitrazepam. The computed vibrational wave numbers their relative IR intensities and the characterization established at the various methods are collected in Table 3. The observed FTIR and FTRaman frequencies for various modes of vibrations are presented in Table 2. Computed scaled values and assignments are presented in Table 4. The relative intensities were obtained by dividing the computed value by the intensity of the strongest line. The observed FTIR and FTRaman spectra are given in figs 1 and 2. The computed intensities show marked deviations from the observed values. One may note that the computed wave numbers correspond to the isolated molecular state whereas the observed wave numbers correspond to the solid-state spectra.

Nitrazepam has three groups (a) a benzene ring with NO_2 group (b) diazepine (c) and a phenyl ring. We have assigned the fundamental modes of these groups on the basis of group vibrational concept and calculated vibrational frequencies. The fundamental vibrational modes were calculated on the basis of DFT and semi empirical calculations. Chemcraft (30) which is a

graphical interface was used to assign the calculated harmonic frequencies using displacement vectors to identify the motions of the atoms. On the whole, the predicted vibrational frequencies are in agreement with the experimental results. The calculated vibrational wave numbers using different methods were compared with experimentally observed values. Some bands found in the predicated IR spectra were not observed in the experimental spectrum of Nitrazepam. The correlation graphs between the unscaled calculated and observed results for the assigned fundamentals in the fingerprint region (500-1700 cm^{-1}) are shown in fig 4. Theoretical harmonic frequencies typically overestimate observed fundamentals due to the neglect of mechanical anhormonicity, electron correlation and basis set effects. Theoretical harmonic frequencies are often scaled to compare with experimental wave numbers. Unscaled harmonic frequencies show a tendency to overestimate experimental fundamentals by more than $140cm^{-1}$. The root mean square deviation of vibrations in the 500-1700 cm^{-1} range is $27.39cm^{-1}$ for BLYP/6-31G(d) and $42.27cm^{-1}$ for B3LYP/6-31G(d). In a second step an overall scaling factor has been applied to the calculated frequencies for these levels. The scaling factor is 1 for the BLYP method and 0.9806 (31) for the B3LYP functional. With use of the scaling factor the root mean square deviation decreased to $25.55cm^{-1}$ for B3LYP. For the better comparison between experimental and theoretical IR wave numbers the plots are drawn, pure Lorentzian band shapes were used with a band width of $10cm^{-1}$, and shown in fig 5. All the bands are well predicted with experimental values.

4.2.1 Vibrational assignments

The present molecule Nitrazepam has C_1 point group symmetry. The molecule has 32 atoms and 90 normal modes of fundamental vibrations span the irreducible representation: 90 A'. All the 90 fundamental vibrations are active in both IR and Raman. The observed FTIR and FTRaman frequencies for various modes of vibrations are presented in table 2.

***Methylene vibrations*:** For the assignments of CH_2 group frequencies, basically six fundamentals can be associated to each CH_2 group, namely CH_2 symmetric stretch; CH_2 asymmetric stretch; CH_2 scissoring and CH_2 rocking which belong to in-plane vibrations. In addition to this two out-of-plane vibrations viz., CH_2 wagging and CH_2 twisting modes, which are expected to be depolarized. The asymmetric stretching vibrations are generally observed in the region 3000 – 2900 cm^{-1}, while the symmetric stretch will appear between 2900 – 2850 cm^{-1} (32). The CH_2 asymmetric vibrations were observed in IR and Raman spectra at 2917 cm^{-1} and 2850 cm^{-1} respectively. The bands corresponding to scissoring and bending vibrations of CH_2 group are presented in table 4.

***C=O vibrations*:** The carbonyl stretching frequency is very sensitive to the factors that disturb the nature of the carbonyl group and its precise frequency is characteristic of the type of the carbonyl compound being studied. Particularly detailed correlations have been made for the carbonyl bond stretching frequency. The carbonyl stretching frequency has been extensively studied by infrared spectroscopy. This multiply bonded group is highly polar ($>C^{\delta+}=O^{\delta-}$) and therefore gives rise to an intense infrared absorption band. The carbon-oxygen double bond is formed by the pπ- pπ bonding between carbon and oxygen. Because of the different electro-negatives of carbon and oxygen atoms, the bonding electrons are not equally distributed between the two atoms. The following two resonance forms contribute to the bonding of the carbonyl group $>C=O \leftrightarrow >C^{+}\text{-}O^{-}$. The lone pair of electrons on oxygen also determines the nature of the carbonyl group. The position of the C=O stretching vibration is very sensitive to various factors such as the physical state, electronic effects by substituents, ring strains, etc. (32). Consideration of these factors provides further information about the environment of the C=O group. The carbonyl stretching generally occurs as a strong absorption in the region 1730 to 1645 cm^{-1}. Sundaraganesan et al. (33) assigned the strong absorption band in FT-IR spectrum at 1688 cm^{-1} correspond to C=O stretching vibration. Accordingly in the present investigation, the peak identified at 1682 cm^{-1} had been assigned to C=O stretching vibration. The scaled value 1682 cm^{-1} in B3LYP/6-31G(d) shows excellent agreement with the experimental value.

***C-C vibrations*:** The C-C stretching (ring) vibrations have given rise to characteristics bands in both the observed IR and Raman spectra, covering the spectral range from 1610 – 1300 cm^{-1}. The IR bands are 1660, 1573, 1507, 1455, 1340 and 1315 cm^{-1}; the Raman bands: 1590, 1498, 1450 and 1337 cm^{-1}. The computed scaled values at 1703, 1622, 1601, 1592, 1505 and 1491 cm^{-1} in B3LYP/6-31G have been assigned to CC stretching vibrations which shows satisfactorily in agreement with experimental values (34). The CC ring breathing mode and C-C-C trigonal bending are assigned to the bands at 863 and 1004 cm^{-1}. The ring breathing mode at 838 cm^{-1} coincides satisfactorily with FTIR band at 863 cm^{-1}. The theoretically computed value of CCC trigonal bending vibrational mode 1004 cm^{-1} exactly matches with weak FTIR band at 1004 cm^{-1}. These assignments are in good agreement with literature value (35). The ring in-plane bending modes have given rise to weak bands across the low-wavenumber region lies less than 1000 cm^{-1}. A very strong band in IR observed at 669 cm^{-1} is due to ring deformation and a predicted band at B3LYP is 681 cm^{-1}. The ring stretching and ring out-of-plane modes have appeared as a series of weak bands in the measured spectral range 700 to 100 cm^{-1}.

NO_2 vibrations: The predicted frequency 118 cm^{-1} (mode no. 6) (NO_2 torsion vibration) is lower by about ~58 cm^{-1} from experimental value. This can be explained by the fact that the presence of hydrogen bonding in Nitrazepam

which imposes some constraint on the torsional motion around the CN bond. The deformation vibrations of NO_2 group (rocking, wagging and twisting) contribute to several normal modes in the low frequency region. It follows from table 4 that the band observed at 508 cm^{-1} corresponds to NO_2 to rocking vibration while theoretically computed value gives rise to 381 cm^{-1}. The NO_2 wagging vibration contributes mainly to the normal mode at 748 cm^{-1} is almost coincides with experimental values of 724 cm^{-1} in FTIR spectrum. A medium strong band at 778 cm^{-1} in FTIR spectrum is assignable to NO_2 scissoring mode. The theoretically calculated value at 833 cm^{-1} is almost coincides with experimental value. Aromatic nitro compounds have absorption due to the asymmetric and symmetric stretching virbrations of the NO_2 to group at 1570 – 1485 and 1370 – 1320 cm^{-1} regions, respectively. Hydrogen bonding has little effect on the NO_2 asymmetric stretching vibrations (34, 36). The bands at 1359 cm^{-1} and 1530 cm^{-1} corresponds to symmetric and asymmetric stretching of NO_2 group, respectively. The theoretically computed value of 1403 and 1522 cm^{-1} satisfactorily coincides with experimental results of NO_2 symmetric and asymmetric stretching. The above results are in good agreement with the literature value (37).

N-H vibrations*:* Tsuboi (38) reported the N-H stretching frequency at 3481cm^{-1} in aniline. In line with his observation N-H stretching is assigned to the band at 3527 cm^{-1} in the present work. The theoretically calculated value by B3LYP/6-31G(d) at 3516 cm^{-1} (mode no. 90) shows excellent agreement with experimentally observed FTIR value at 3527 cm^{-1}. The N-H in-plane bending and N-H out-of-plane bending are assigned to the bands at 1507 and 631 cm^{-1} which agrees well with Venkateswaran and Pandya (39) and Evans (40). The calculated value for N-H out-of-plane bending vibration at 639 cm^{-1} (mode no.26) is in excellent agreement with experimental observation. However, the theoretical value for the N-H in-plane bending vibration at 1259 cm^{-1} deviates negatively by ~ 248 cm^{-1} from experimental observation may be coupled with C-H in-plane bending vibration.

C=N, C-N vibrations: The identification of the C-N stetching frequency in the side chains is a task since there are problems in identifying these frequencies from other vibrations. Silverstein et al. (41) assigned C-N stretching absorption in the region 1382 – 1266 cm^{-1} for aromatic amines. In benzamide the band observed at 1368 cm^{-1} is assigned to be due to C-N stretching (42). Sundaraganesan et al (43) had assigned the C-N stretching of 2,4-dinitro phenyl hydrazine at 1335 cm^{-1} in FTRaman spectrum. Kahovec and Kohlreusch (44) identified the stretching vibration of C=N band in salicyclic aldoxime at 1617 cm^{-1}. Referring to the above workers the bands at 1389 cm^{-1} and 1620 cm^{-1} in FTIR spectrum have been assigned to C-N and C=N stretching, respectively. The theoretically computed value of C-N stretching vibration at 1369 cm^{-1} (mode no. 66) and for C=N stretching vibration at 1634cm^{-1} (mode no. 78) exactly matches with experimental value.

5. Conclusion

The frequency assignments were performed from FT-IR spectrum recorded for Nitrazepam. Theoretical DFT and semi empirical calculations of the vibrational spectra of the molecule presented in this paper are compared with the experimental spectrum of the compound Nitrazepam. Geometries were reproduced within the limits of accuracy of available experimental data. All frequencies of the bands can be approached practically by theoretical calculation performed for a single isolated molecule. Regarding the geometries and the harmonic vibrational frequencies, we found that B3LYP/6-31G(d) is better.

Table 1. Bond lengths (Å) and angles (°) values for Nitrazepam

Parameters	AM1	PM3	BLYP	B3LYP	Experimental
Bond length (Å)					
R(1-2)	1.240	1.217	1.252	1.239	1.225
R(2-3)	1.397	1.435	1.413	1.396	1.427
R(2-21)	1.524	1.517	1.533	1.519	1.517
R(3-4)	1.395	1.429	1.414	1.403	1.428
R(3-22)	1.002	1.000	1.023	1.014	1.022
R(4-5)	1.424	1.407	1.425	1.413	1.420
R(4-12)	1.418	1.407	1.436	1.422	1.429
R(5-6)	1.382	1.383	1.396	1.386	1.403
R(5-23)	1.103	1.099	1.093	1.085	1.090
R(6-7)	1.407	1.403	1.411	1.400	1.406
R(6-24)	1.105	1.100	1.089	1.082	1.088
R(7-8)	1.484	1.497	1.477	1.460	1.470
R(7-11)	1.398	1.395	1.402	1.391	1.406
R(8-9)	1.202	1.215	1.288	1.265	1.316
R(8-10)	1.202	1.215	1.289	1.266	1.316

R(11-12)	1.400	1.397	1.416	1.405	1.415
R(11-25)	1.107	1.104	1.088	1.082	1.088
R(12-13)	1.482	1.478	1.503	1.494	1.494
R(13-14)	1.485	1.482	1.501	1.492	1.495
R(13-20)	1.293	1.294	1.314	1.298	1.297
R(14-15)	1.400	1.396	1.421	1.409	1.414
R(14-19)	1.401	1.395	1.420	1.408	1.406
R(15-16)	1.395	1.391	1.405	1.395	1.406
R(15-26)	1.101	1.096	1.091	1.083	1.090
R(16-17)	1.394	1.391	1.412	1.402	1.405
R(16-27)	1.100	1.095	1.093	1.085	1.090
R(17-18)	1.396	1.391	1.409	1.399	1.406
R(17-28)	1.100	1.095	1.093	1.085	1.085
R(18-19)	1.393	1.391	1.409	1.399	1.406
R(18-29)	1.100	1.095	1.093	1.085	1.085
R(19-30)	1.100	1.095	1.091	1.084	1.084
R(20-21)	1.429	1.456	1.487	1.471	1.453
R(21-31)	1.131	1.109	1.096	1.089	1.100
R(21-32)	1.129	1.110	1.110	1.102	1.100
		Bond angles (°)			
A(1-2-3)	118.10	115.10	120.50	120.60	120.50
A(1-2-21)	122.10	124.20	124.70	124.30	122.60
A(3-2-21)	119.80	120.60	114.80	115.10	120.00
A(2-3-4)	126.40	122.30	128.30	128.20	128.00
A(2-3-22)	115.50	115.10	113.30	113.50	118.00
A(2-21-20)	115.30	113.40	111.10	110.90	118.00
A(2-21-31)	106.90	110.20	107.40	107.40	118.00
A(2-21-32)	107.80	109.60	108.90	109.00	120.00
A(4-3-22)	115.80	113.40	117.20	117.40	120.00
A(3-4-5)	118.00	118.20	117.40	117.40	120.00
A(3-4-12)	123.50	122.30	122.60	122.70	120.00
A(5-4-12)	118.50	119.40	119.90	119.90	120.00
A(4-5-6)	121.40	120.70	121.20	121.20	119.19
A(4-5-23)	119.90	120.50	118.90	119.00	120.00
A(4-12-11)	119.80	119.30	117.90	118.10	120.00
A(4-12-13)	122.80	122.70	122.50	122.40	119.98
A(6-5-23)	118.70	118.80	119.80	119.80	120.00
A(5-6-7)	119.40	119.90	118.50	118.50	119.98
A(5-6-24)	120.50	119.50	121.80	121.80	120.00
A(7-6-24)	120.20	120.60	119.70	119.80	120.00
A(6-7-8)	119.70	120.10	119.20	119.20	120.00
A(6-7-11)	120.40	119.60	121.60	121.60	120.00
A(8-7-11)	120.00	120.20	119.20	119.20	120.00
A(7-8-9)	119.00	119.30	118.10	118.20	120.00
A(7-8-10)	118.80	119.30	117.80	117.90	120.00
A(7-11-12)	120.50	120.90	120.80	120.60	120.00
A(7-11-25)	120.10	120.80	118.90	119.10	120.00
A(9-8-10)	122.20	121.40	124.10	123.90	120.00
A(12-11-25)	119.40	118.30	120.30	120.30	123.22
A(11-12-13)	117.50	117.90	119.50	119.40	116.99
A(12-13-14)	114.50	116.90	118.80	118.70	120.00
A(12-13-20)	126.80	125.40	124.70	124.40	120.00
A(14-13-20)	118.70	117.70	116.40	116.80	120.00
A(13-14-15)	120.40	120.20	119.10	119.00	120.00
A(13-14-19)	119.70	119.50	122.20	122.10	120.00
A(13-20-21)	122.30	123.70	119.70	120.20	120.00

A(15-14-19)	119.90	120.30	118.60	118.80	119.98
A(14-15-16)	119.80	119.70	120.60	120.60	120.00
A(14-15-26)	120.10	120.30	118.40	118.40	120.00
A(14-19-18)	119.90	119.70	120.60	120.60	119.98
A(14-19-30)	120.00	120.20	120.10	120.10	120.00
A(16-15-26)	120.00	120.10	121.00	121.00	120.00
A(15-16-17)	120.20	120.20	120.30	120.20	120.00
A(15-16-27)	119.70	119.80	119.70	119.70	120.00
A(17-16-27)	120.10	120.00	120.00	120.00	120.00
A(16-17-18)	120.00	120.10	119.70	119.70	120.00
A(16-17-28)	120.10	120.00	120.20	120.20	120.00
A(18-17-28)	120.00	120.00	120.20	120.10	120.00
A(17-18-19)	120.10	120.20	120.20	120.20	123.00
A(17-18-29)	120.10	120.00	120.20	120.20	110.90
A(19-18-29)	119.80	119.80	119.60	119.70	108.00
A(18-19-30)	120.10	120.10	119.30	119.30	108.00
A(20-21-31)	106.20	105.50	108.50	108.70	105.91
A(20-21-32)	112.10	111.10	111.80	111.80	101.42
A(31-21-32)	108.20	106.80	109.00	108.90	106.00

Table 2. Experimental FTIR and FTRaman frequencies and assignments for Nitrazepam.

Species	FTIR frequency and intensity	FTRaman frequency and intensity	Vibrational assignments
	3677		(2362+1315)
A'	3527w	3525vw	N-H stretch
A'	3380w	3381w	C-H stretch
A'	3344w	3340vw	C-H stretch
A'	3260w	3279w	C-H stretch
A'	2977s	2980w	C-H stretch
A'	2932w		C-H stretch
A'	2917w		CH_2 asym stretch
A'	2900s		C-H stretch
A'	2850w	2878vs	CH2 sym stretch
	2362		1359±1004
A'	1682w	1680vw	C=O stretch
A'	1660vw		C=C stretch
A'	1620w	1601w	C=N stretch
A'	1573w	1590w	C=C stretch
A'	1530vw	1544vw	NO_2 asym stretch
A'	1507vw	1498vw	C=C stretch
A'	1469m		CH_2 scissoring
A'	1455w	1450m	CH_2 deform
A'	1433w	1423w	CH_2 deform
A'	1395w		CH_2 deform
A'	1389m	1377vw	C-N stretch
A'	1377w		CH_2 stretch
A'	1359m		NO_2 sym stretch
A'	1341s	1337vs	CH ipb
A'	1315s		CH ipb
A'	1296w		CH_2 wagging
A'	1250s	1260m	NH ipb
A'	1210w		CH ipb
A'	1167m		CH_2 twisting

A'	1142w		CH ipb
A'	1115m	1120m	CH ipb
A'	1090w	1095w	C-C-C bending
A'	1083w		CH ipb
A'	1071w		CH ipb
A'	1057w		CH ipb
A'	1034m	1038vw	CH ipb
A'	1019w	1025vw	CH ipb
A'	1004m	1005vw	C-C-C trigonal bending
A'	988m	962vw	CH opb
A'	915m	910w	CH opb
A'	899vs		CH opb
A'	838w	853w	CC ring breathing
A'	778w	776vw	NO_2 scissoring
A'	750w		CH opb
A'	724w	733vw	NO_2 wagging
A'	702w	693vw	CH_2 rocking
A'	669m		C-C-C ipb
A'	631w	637w	NH opb
A'	604m		ONO bending
A'	566w		CCC ipb
A'	551s	550w	CCC ipb
A'	516w		CCC opb
A'	508w	496w	NO_2 rocking
A'		470s	CCC opb
A'		431w	CCC opb
A'		360s	CCC opb
A'		252w	CCC opb
A'		202w	C-NO_2 opb
A'		176s	NO_2 torsion

ipb – in-plane bending; opb – out of plane bending; asym – asymmetric; sym – symmetric.

Table 3. Calculated unscaled IR wavenumbers (relative intensities) for Nitrazepam using B3LYP, BLYP, AM1 and PM3 methods.

Species	AM1		PM3		BLYP/6-31G(d)		B3LYP/6-31G(d)	
W1(A)	21	0	23	0	40	0	41	0
W2(A)	36	0	29	0	52	0	53	0
W3(A)	43	0	44	0	53	0	55	0
W4(A)	58	0	54	0	67	1	69	1
W5(A)	71	0	61	0	85	0	86	0
W6(A)	110	1	101	1	117	1	121	1
W7(A)	120	0	116	0	146	0	152	0
W8(A)	168	0	165	0	167	1	174	1
W9(A)	184	0	176	0	208	0	215	0
W10(A)	248	0	236	0	248	0	256	0
W11(A)	262	0	248	0	261	1	271	1
W12(A)	298	1	285	1	296	1	308	1
W13(A)	325	0	297	0	305	1	318	1
W14(A)	349	0	322	0	324	0	337	0
W15(A)	366	0	346	0	374	1	389	1
W16(A)	370	0	356	0	409	1	423	0

W17(A)	437	1	422	0	412	0	427	0
W18(A)	465	1	438	0	435	0	452	0
W19(A)	478	1	445	2	458	0	475	0
W20(A)	494	3	458	2	482	1	502	1
W21(A)	510	0	495	0	503	1	523	1
W22(A)	546	0	535	0	533	1	554	2
W23(A)	594	2	550	0	539	1	561	1
W24(A)	605	22	563	0	567	1	589	1
W25(A)	616	2	604	8	603	7	626	7
W26(A)	646	1	625	0	633	1	652	0
W27(A)	657	0	641	6	644	4	674	5
W28(A)	670	1	650	1	667	1	694	2
W29(A)	698	6	669	7	686	7	710	6
W30(A)	742	5	701	10	692	0	724	4
W31(A)	764	8	722	6	702	6	730	3
W32(A)	771	8	755	14	719	6	751	5
W33(A)	800	2	768	27	726	7	763	9
W34(A)	825	1	778	3	750	9	784	11
W35(A)	842	15	783	7	791	2	824	2
W36(A)	889	0	833	4	810	1	849	2
W37(A)	890	6	848	0	840	9	880	9
W38(A)	924	4	876	1	850	1	884	2
W39(A)	958	0	912	1	852	1	893	2
W40(A)	972	0	937	0	888	1	927	1
W41(A)	989	1	946	2	925	0	971	1
W42(A)	990	2	965	3	930	2	973	1
W43(A)	994	0	976	3	947	3	994	3
W44(A)	1010	0	978	0	964	0	1011	0
W45(A)	1029	0	1001	9	973	0	1022	0
W46(A)	1049	1	1007	2	974	2	1024	2
W47(A)	1081	5	1018	0	992	0	1035	1
W48(A)	1124	2	1026	1	1002	3	1040	1
W49(A)	1151	0	1059	0	1011	6	1047	5
W50(A)	1170	0	1086	2	1035	1	1069	1
W51(A)	1188	0	1098	0	1084	7	1128	5
W52(A)	1197	0	1130	1	1095	1	1132	4
W53(A)	1228	1	1150	0	1136	6	1181	2
W54(A)	1231	0	1151	0	1153	18	1198	8
W55(A)	1249	0	1180	1	1180	100	1224	0
W56(A)	1273	12	1189	9	1193	11	1236	9
W57(A)	1315	0	1215	0	1194	0	1239	1
W58(A)	1324	0	1235	3	1206	3	1277	98
W59(A)	1353	1	1276	15	1236	3	1284	4
W60(A)	1369	1	1293	17	1254	19	1312	26
W61(A)	1375	1	1304	0	1279	1	1327	3
W62(A)	1391	1	1328	4	1285	23	1347	21
W63(A)	1449	3	1344	8	1321	4	1365	3
W64(A)	1465	7	1361	1	1330	0	1370	2
W65(A)	1484	7	1382	1	1332	20	1389	0
W66(A)	1499	22	1415	28	1350	1	1397	9
W67(A)	1547	16	1449	27	1355	4	1431	5
W68(A)	1566	3	1536	1	1392	4	1467	19
W69(A)	1625	7	1565	10	1455	5	1505	2
W70(A)	1634	5	1599	73	1458	3	1520	10
W71(A)	1687	84	1602	28	1483	3	1535	3
W72(A)	1744	32	1625	3	1493	2	1541	2

W73(A)	1753	52	1762	8	1502	0	1552	0
W74(A)	1763	0	1777	0	1540	7	1624	4
W75(A)	1774	0	1788	25	1566	11	1633	5
W76(A)	1799	5	1796	1	1576	9	1654	11
W77(A)	1945	7	1875	10	1587	18	1659	23
W78(A)	2016	100	1898	100	1595	0	1666	6
W79(A)	2059	70	1942	76	1658	86	1737	100
W80(A)	2962	3	2929	1	2918	6	3005	5
W81(A)	3031	7	2985	9	3087	3	3171	2
W82(A)	3134	14	2996	4	3113	0	3197	0
W83(A)	3154	11	3022	4	3123	2	3207	2
W84(A)	3173	13	3041	9	3127	2	3213	1
W85(A)	3181	1	3054	0	3135	9	3218	7
W86(A)	3182	1	3056	0	3146	4	3229	4
W87(A)	3186	8	3063	4	3160	2	3243	1
W88(A)	3191	17	3070	9	3184	0	3265	1
W89(A)	3199	5	3079	3	3185	1	3266	1
W90(A)	3412	25	3343	3	3467	5	3586	8

Table 4. Experimental and calculated scaled IR wavenumbers for Nitrazepam using B3LYP, BLYP, AM1 and PM3 methods.

Species	AM1	PM3	BLYP/ 6-31G(d)	B3LYP/ 6-31G(d)	Assignments
W1(A)	20	22	41	40	Phenyl ring butterfly
W2(A)	34	28	53	52	Phenyl ring butterfly
W3(A)	41	43	54	54	Phenyl ring butterfly
W4(A)	55	53	68	68	Phenyl ring floating
W5(A)	68	60	86	84	Ring torsion
W6(A)	105	99	118	119	NO_2 torsion
W7(A)	114	113	148	149	CH_2 wagging + γNH
W8(A)	160	161	169	171	Phenyl ring floating
W9(A)	175	172	211	211	CH_2 wagging
W10(A)	236	230	251	251	Phenyl ring floating
W11(A)	250	242	264	266	Ring torsion
W12(A)	284	278	300	302	CH_2 wagging
W13(A)	310	290	309	312	CH_2 wagging
W14(A)	333	314	328	330	γCCH+γCCO
W15(A)	349	338	379	381	NO_2 rocking
W16(A)	353	347	414	415	γCCH
W17(A)	417	412	417	419	Ring wagging
W18(A)	443	428	440	443	γHCH
W19(A)	456	434	464	466	γCCH
W20(A)	471	447	488	492	γCCH
W21(A)	486	483	509	513	δCCN
W22(A)	520	522	540	543	γCCC+δring
W23(A)	566	537	546	550	δCCC+γNC=O+δCCN
W24(A)	577	550	574	578	γCCC+ δring
W25(A)	587	590	611	614	δONO
W26(A)	616	610	641	639	γNH
W27(A)	626	626	652	661	Ring deformation

W28(A)	639	634	675	681	δCCC + δring
W29(A)	665	653	695	696	Ring puckering
W30(A)	707	684	701	710	CH_2 rocking + γCH
W31(A)	728	705	711	716	γCH
W32(A)	735	737	728	736	γCH
W33(A)	763	750	735	748	NO_2 wagging
W34(A)	786	759	759	769	γCH
W35(A)	803	764	801	808	γCH
W36(A)	847	813	820	833	NO_2 scissoring
W37(A)	848	828	851	863	C-C ring breathing
W38(A)	881	855	861	867	δCCN
W39(A)	913	890	863	876	γCH
W40(A)	927	915	899	909	δCNH+δNCO
W41(A)	943	923	937	952	γCH+ δCCN
W42(A)	944	942	942	954	Ring deformation
W43(A)	947	953	959	975	γCH
W44(A)	963	955	976	991	γCH
W45(A)	981	977	985	1002	γCCC+γCH
W46(A)	1000	983	986	1004	CCC trigonal bending
W47(A)	1030	994	1004	1015	δCH
W48(A)	1071	1001	1015	1020	δCH
W49(A)	1097	1034	1024	1027	δCH
W50(A)	1115	1060	1048	1048	δCH
W51(A)	1132	1072	1098	1106	δCH
W52(A)	1141	1103	1109	1110	δCCH+δCCC
W53(A)	1171	1123	1150	1158	δCH
W54(A)	1173	1123	1168	1175	δC-N+δNO_2
W55(A)	1191	1152	1195	1200	δCH
W56(A)	1213	1161	1208	1212	tCH_2+δCH
W57(A)	1253	1186	1209	1215	δCCH
W58(A)	1262	1205	1221	1252	δCN
W59(A)	1290	1246	1252	1259	νC-N
W60(A)	1305	1262	1270	1287	δCH
W61(A)	1311	1273	1295	1301	δCCH
W62(A)	1326	1296	1301	1321	ωCH_2+δCH
W63(A)	1381	1312	1338	1339	δCH_2
W64(A)	1396	1328	1347	1343	δCH_2+CCH
W65(A)	1415	1349	1349	1362	δCCH
W66(A)	1429	1381	1367	1370	νC-N
W67(A)	1475	1414	1372	1403	ν_{sym} NO_2
W68(A)	1493	1499	1410	1439	Ring deformation
W69(A)	1549	1528	1473	1476	CH_2 scissoring
W70(A)	1558	1561	1476	1491	νC=C
W71(A)	1608	1564	1502	1505	νC=C
W72(A)	1662	1586	1512	1511	δNH
W73(A)	1671	1720	1521	1522	$\nu_{asym}NO_2$

W74(A)	1680	1735	1559	1592	νC=C
W75(A)	1691	1745	1586	1601	νC=C
W76(A)	1715	1753	1596	1622	νC=C
W77(A)	1854	1830	1607	1627	νC=N
W78(A)	1922	1853	1615	1634	νC=O
W79(A)	1963	1896	1679	1703	νC=C
W80(A)	2823	2859	2955	2947	$\nu_{sym}CH_2$
W81(A)	2889	2914	3126	3109	νCH
W82(A)	2987	2924	3152	3135	ν_{asym} CH_2
W83(A)	3006	2950	3162	3145	νCH
W84(A)	3025	2968	3166	3151	νCH
W85(A)	3032	2981	3175	3156	νCH
W86(A)	3033	2983	3186	3166	νCH
W87(A)	3037	2990	3200	3180	νCH
W88(A)	3042	2997	3224	3202	νCH
W89(A)	3049	3005	3225	3203	νCH
W90(A)	3252	3263	3511	3516	νNH

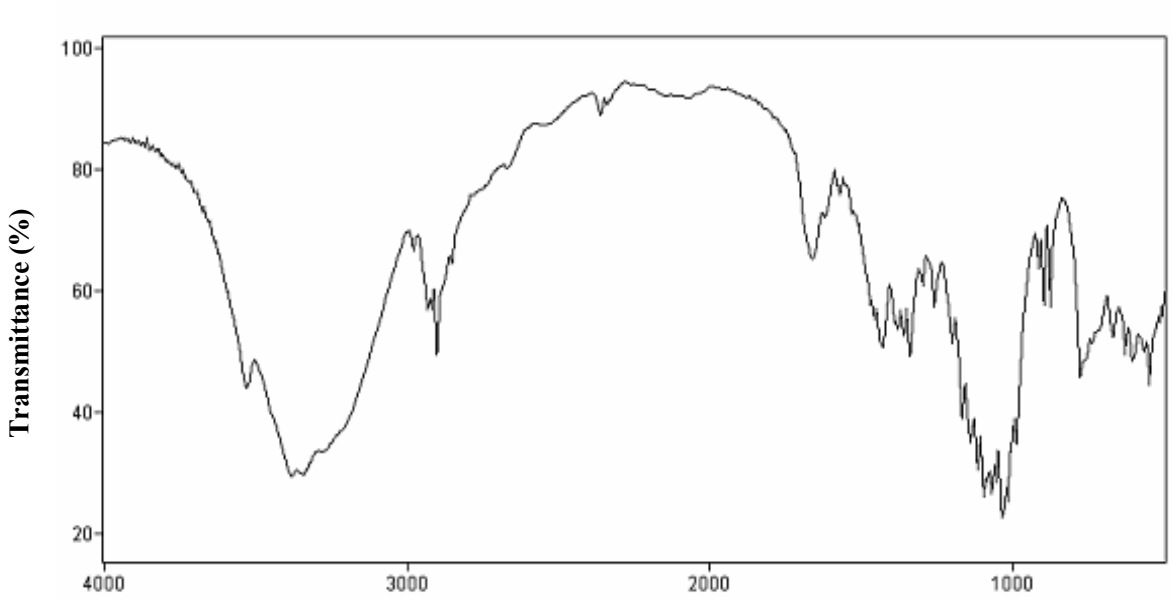

Figure 1. FTIR spectrum of Nitrazepam

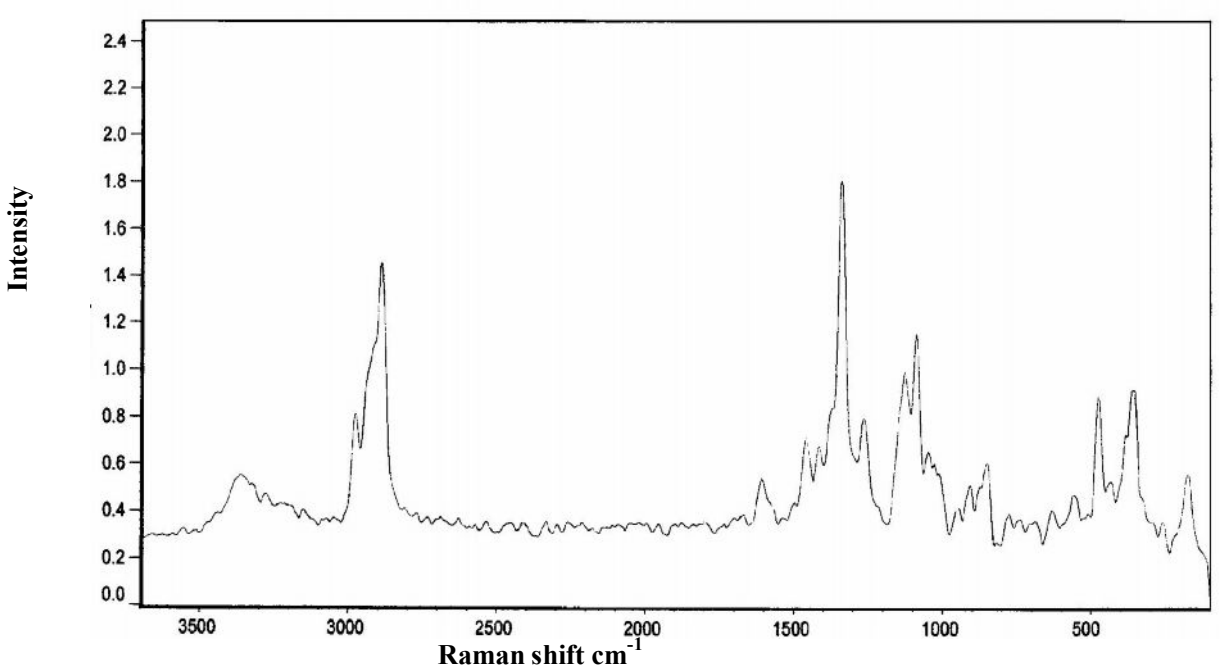

Figure 2. FTRaman Spectrum of Nitrazepam

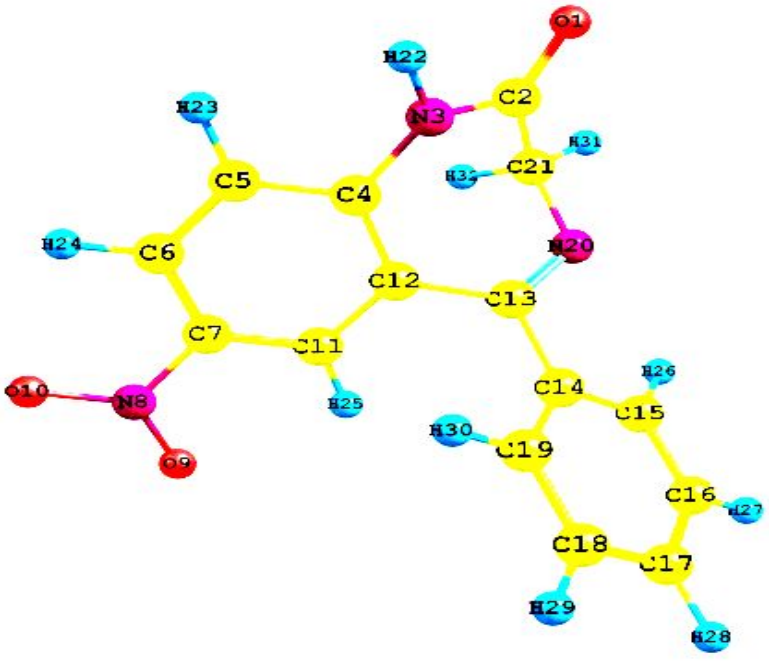

Figure 3. Optimized structure of Nitrazepam using B3LYP/6-31G(d)

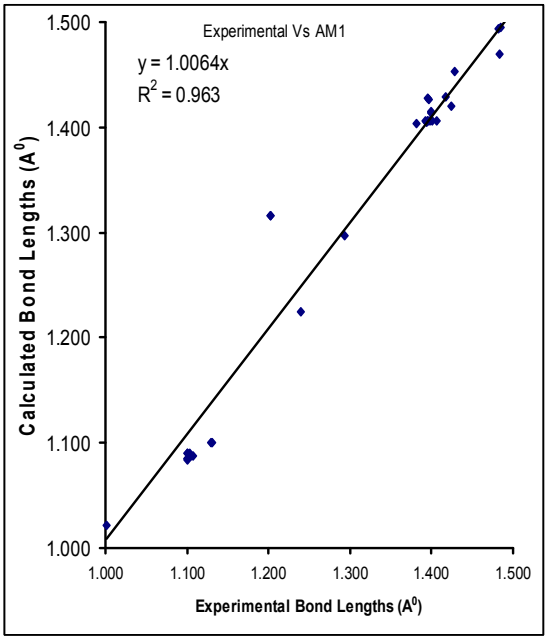

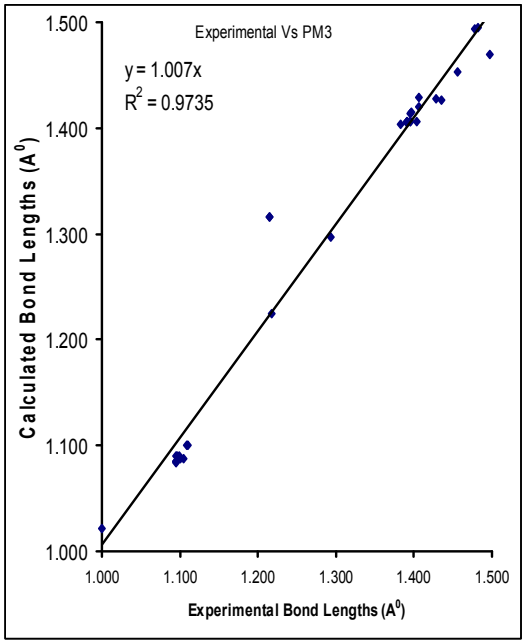

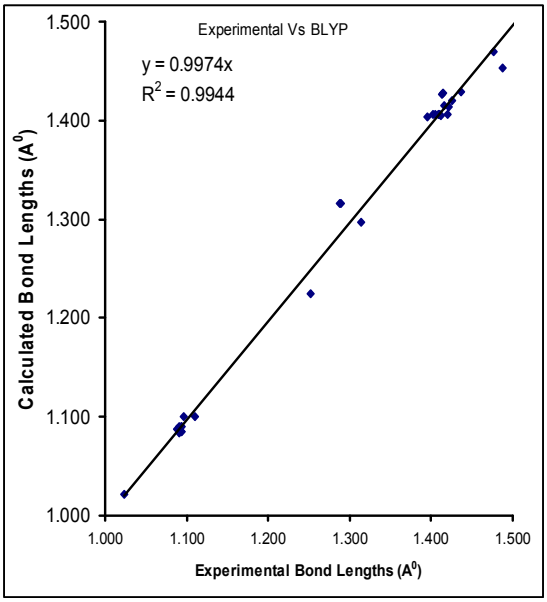

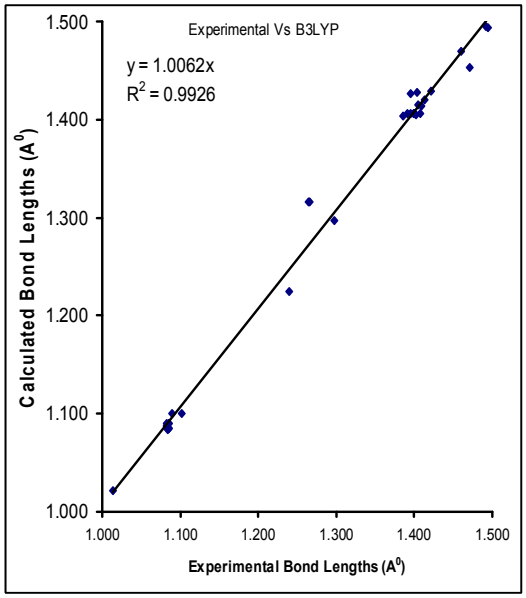

Figure 4a. Correlation graph of Melatonin for computed geometrical parameters versus experimental

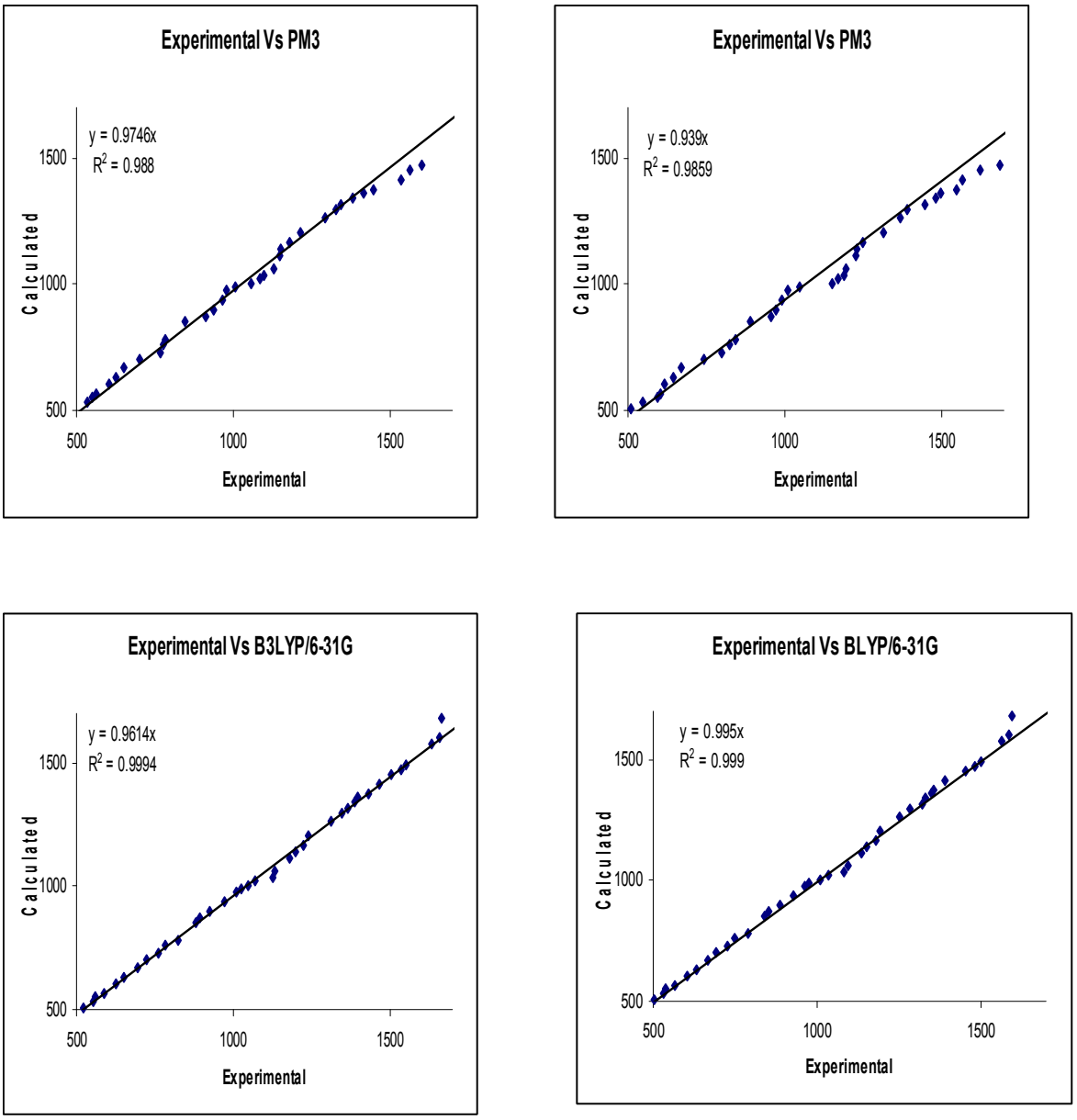

Figure 4b. Correlation graph of Melatonin for computed unscaled and experimental wavenumbers

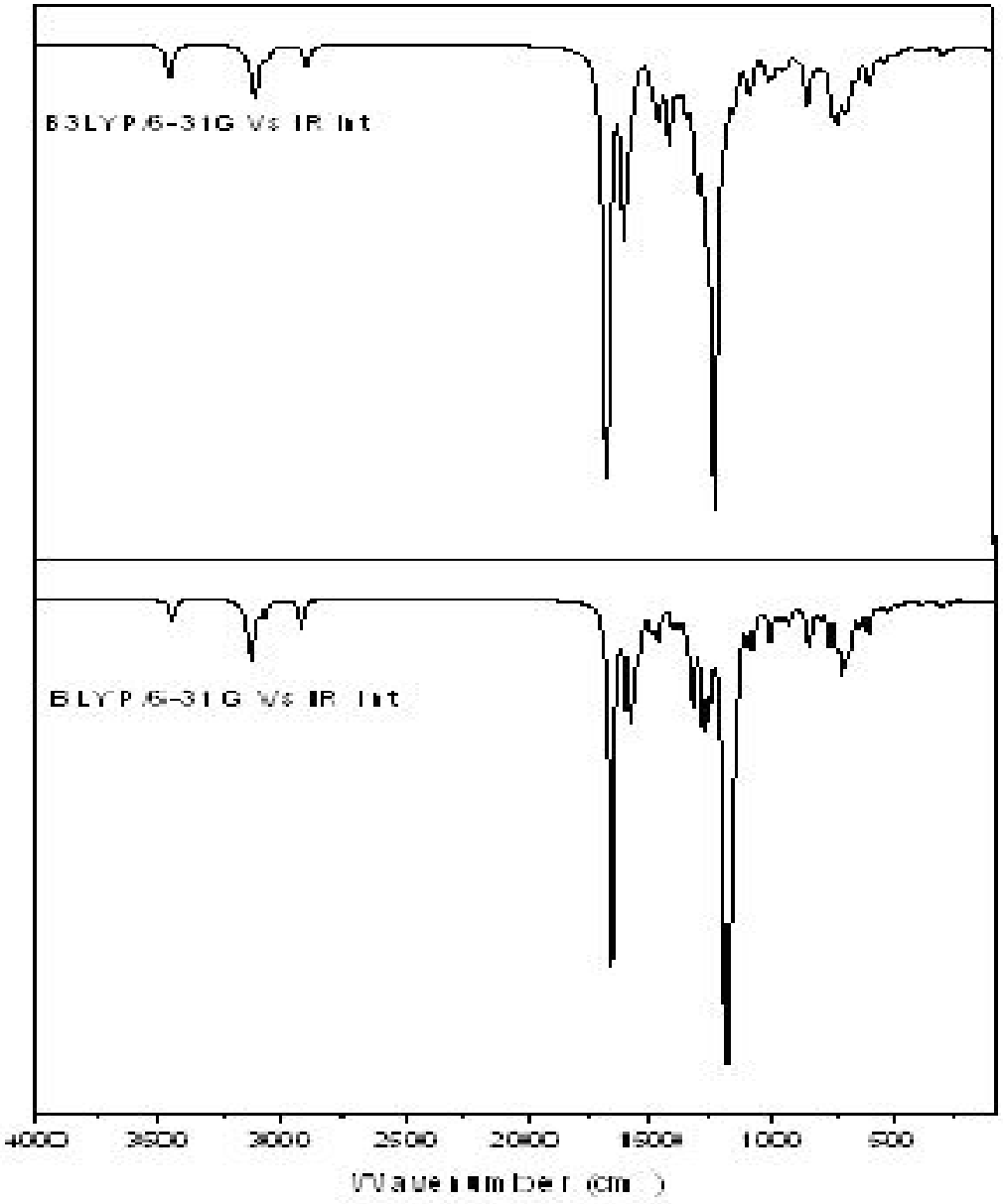

Figure 5. Computed IR spectrum of Nitrazepam at BLYP and B3LYP levels using 6-31G(d) basis set

References

1. M.C.Gravielle, R.Faris, S.J.Russek, S.H.Farb, J.Biol. Chem. 280, 20954 (2005).
2. S.I.Wikinski, G.B.Acosta, M.C.Gravielle, C.D. Bonavita, V.Bisango, S.Fiszer-Plazas, M.C.Rubio, Pharmacol.Biochem.Behav. 68, 721 (2001).
3. D.J.Greenblatt, J.S.Harmatz, R.I.Shader, Clin.P harmacokinet. 21,165 (1991).
4. B.G.Katzung, Basic and Clinical Pharmacology, Medical Publishing Division, London, 2004.
5. M.Fukinaga, K.Ishizawa, K.C.Kamei, Pharmacology. 57, 233 (1998).
6. W.B.Mendelson, Psychiatr.Dev.2(1984)161.
7. J.F.Liegeois, L.Eyrolles, B.A.Ellenbrock, C.Lejeune, P.Carato, J.Bruthwyler, J.Geczy, J.Damas,J.Delarge, J.Med.Chem.45(2002)5136.
8. P.Giusti,R.Arban, Pharmacol.Res.27(1993)201.
9. P.Giusti, G.Guidetti, E.Costa, A.Guidotti, J.Pharmacol.Exp.Ther.257(1991) 1062.
10. K.D.Tripathi, medical Pharmacology, Jaypee Brothers Medical Publishers,New Delhi (1995).

11. Indian Pharmacopoeia, Controller of Publication, civil Lines, Delhi, Vol.I And II (1996).
12. A.Ravi-Kreeti, B. Ashok-Kumar,T.Partha - sarathy, V.Uma, Bioorg. Med. Chem.13(2005)1873.
13. A.Lu,J.Zhou,J.Chem.Inf.Comput.Sci.44(2004) 1130.
14. J.Kawakami,K.Hoshi,A.Ishiyama, S.Miyagishima,K.Sato,Chem.Pharm.Bull.52(20 04)751.
15. S.P.Gupta, Curr.Pharm.Des.8(2002)111.
16. D.Berezhnoy, R.Baur, A.Gonthier, B.Foucaud, M.Goeldner,E.Sigel,J.Neurochem.92(2005) 859.
17. L.T.Schove,J.J.Perez,G.H.Loew,Bioorg Med.Chem.2(1994)1029.
18. G.H.Loew, J.R.Nienow, M.Poulsen, Mol.Pharmacol.26(1984)199.
19. G.A.Neville, H.D.Beckstead, H.F.Shurvell, J.Pharm.Sciences. 83(2006)143.
20. S.Gunasekaran, R,Arunbalaji, S.Seshadri & S.Muthu, Indian J. pure& Appl.phys, 46(2008)33.
21. D.C.Young, Computational Chemistry: A Practical Guide for Applying Technique to Real World Problems., John Wiley & Sons Inc., 2001.p.42.
22. V.Chis, S.Filip, V.Miclaus, A.Pirnau, C.Tanaselia, V.Almasan, M.Vasilescu, J.Mol.Struct.744-747(2005)363.
23. www.chemsoft.com
24. Frisch MJ, Trucks GW, Schlegel HB, Scuseria GE, Robb MA, Cheeseman JR, Montgomery JA, Jr., Vreven T, Kudin KN, Burant JC, Millam JM, Iyengar SS, Tomasi J, Barone V, Mennucci B, Cossi M, Scalmani G, Rega N, Petersson GA, Nakatsuji H, Hada M, Ehara M, Toyota K, Fukuda R, Hasegawa J, Ishida M, Nakajima T, Honda Y, Kitao O, Nakai H, Klene M, Li X, Knox JE, Hratchian HP, Cross JB, Bakken V, Adamo C, Jaramillo J, Gomperts R, Stratmann RE, Yazyev O, Austin AJ, Cammi R, Pomelli C, Ochterski JW, Ayala PY, Morokuma K, Voth GA, Salvador P, Dannenberg JJ, Zakrzewski VG, Dapprich S, Daniels AD, Strain MC, Farkas O, Malick DK, Rabuck AD, Raghavachari K, Foresman JB, Ortiz JV, Cui Q, Baboul AG, Clifford S, Cioslowski J, Stefanov BB, Liu G, Liashenko A, Piskorz P, Komaromi I, Martin RL, Fox DJ, Keith T, Al-Laham MA, Peng CY, Nanayakkara A, Challacombe M, Gill PMW, Johnson B, Chen W, Wong MW, Gonzalez C, and Pople JA (2004) Gaussian 03.Gaussian Inc, Wallingford CT
25. M.J.S.Dewar, E.G.Joebisch, E.F.Healy and J.J.P.Stewart, J.Am.Chem.Soc.10(1995)3902.
26. J.J.P.Stewart, J.Comput.Chem.,10(1989)209.
27. B.G.Johnson, P.M.W.Gill, J.A.Pople, J.Chem. Phys.98(1993)5612.
28. A.P.Scott,l.radom, J.Phys.Chem.100(41)(1996)16502.
29. G.Rauhut, P.Pulay, J.Phys. Chem.99(10)(1995)3093.
30. www.Chemcraft.com
31. P.Pulay, G.Fogarasi, G.Pongor, J.E.Boggs, A.Vargha, J.Am.Chem.Soc.105(1983)7037-7047.
32. G.Socrates, Infrared characteristic Group Frequencies, Ist Ed, John Wiley,(1980).
33. N.Sundaraganesan, S.Illakiamani, B.Dominic Joshua, Spectrochim. Acta A1386-1425(2006).
34. L.J. Bellamy, The Infrared Spectra of Complex Molecules, Chapman and Hall, London, 1975.
35. H. Lampert, W. Mikenda, A. Karpfen, J. Phys. Chem. A 101, 268 (1997).
36. D.N. Sathyanarayan, Vibrational Spectroscopy- Theory and Applications, Second Ed., New Age Internations Pvt. Ltd. Publishers, New Delhi, 2004.
37. A.J. Abkowicz-Bienko, Z. Latajka, D.C. Bienko, D. Michaleska, Chem. Phys. 250, 123 (1999).
38. M.Tsuboi, Spectrochim. Acta A16(1960)505.
39. C.S.Venkateshwaran, N.S.Pandya, Proc.Indian Acad.Sci.A15 (1942)390.
40. J.C.Evans, Spectrochim.Acta A16 (1960) 428.
41. R.M.Silverstein, G.Claytonbassler, Torence C.Morrill, Spectrometric Identification of Organic Compounds, 5th Ed, John Wiley, (1997).
42. R. Shanmugam, D. Sathyanarayna, Spectrochim Acta A 40, 764 (1984).
43. N. Sundaraganesan, S. Ayyappan, H. Umamaheswari, B. Dominic Joshua, Spectrochim Acta A 66, 17-27 (2007).
44. L. Kahovec, K.W. F. Kohlreusch, Monatsh. Chem. 74, 333 (1941).

*****